

Broadband extraordinary transmission in a single sub-wavelength aperture

Wenxuan Tang,¹ Yang Hao,^{1,*} and Francisco Medina ²

¹Department of Electronic Engineering, Queen Mary University of London,
Mile End Road, London E1 4NS, UK

²Department Electronics and Electromagnetism, Physics Faculty, University of Seville,
Av. Reina Mercedes s/n, 41012-Seville, Spain

[*yang.hao@elec.qmul.ac.uk](mailto:yang.hao@elec.qmul.ac.uk)

Abstract: Coordinate transformation is applied to design an all-dielectric device for Extraordinary Transmission (ET) in a single sub-wavelength slit. The proposed device has a broadband feature and can be applied from microwave to visible frequency bands. Finite-Difference Time-Domain (FDTD) simulations are used to verify the device's performance. The results show that significantly increased transmission is achieved through the sub-wavelength aperture from 4 GHz to 8 GHz when the device is applied. In contrast with previously reported systems, the frequency sensitivity of the new device is very low.

© 2010 Optical Society of America

OCIS codes: (050.6624) Subwavelength structures; (260.2110) Electromagnetic optics; (350.4010) Microwaves.

References and links

1. T. W. Ebbesen, H. J. Lezec, H. F. Ghaemi, T. Thio and P. A. Wolff, "Extraordinary optical transmission through sub-wavelength hole arrays," *Nature* **391**, 667–669 (1998).
2. J. A. Porto, F. J. García-Vidal and J. B. Pendry, "Transmission resonances on metallic gratings with very narrow slits," *Phys. Rev. Lett.* **83** (14), 2845–2848 (1999).
3. C. Genet and T. W. Ebbesen, "Light in tiny holes," *Nature* **445**, 39–46 (2007).
4. F. J. García-de-Abajo, "Colloquium: Light scattering by particle and hole arrays," *Rev. Mod. Phys.* **79**, 1267–1290 (2007).
5. F. J. García-Vidal, L. Martín-Moreno, T. W. Ebbesen and L. Kuipers, "Light passing through subwavelength apertures," *Rev. Mod. Phys.* **82**, 729–787 (2010).
6. H. J. Lezec, A. Degiron, E. Devaux, R. A. Linke, L. Martín-Moreno, F. J. García-Vidal and T. W. Ebbesen, "Beaming light from a subwavelength aperture," *Science* **297** (5582), 820–822 (2002).
7. F. J. García-Vidal, H. J. Lezec, T. W. Ebbesen and L. Martín-Moreno, "Multiple paths to enhance optical transmission through a single subwavelength slit," *Phys. Rev. Lett.* **90**, 213901 (2003).
8. L. A. Dunbar, M. Guillaumée, F. de León-Pérez, C. Santschi, E. Grenet, R. Eckert, F. López-Tejiera, F. J. García-Vidal, L. Martín-Moreno and R. P. Stanley, "Enhanced transmission from a single subwavelength slit aperture surrounded by grooves on a standard detector," *App. Phys. Lett.* **95**, 011113 (2009).
9. J. B. Pendry, L. Martín-Moreno and F. J. García-Vidal, "Mimicking surface plasmons with structured surfaces," *Science* **305**, 847–848 (2004).
10. K. Aydin, A. O. Cakmak, L. Sahin, F. Bilotti, L. Vegni and E. Ozbay, "Split-ring-resonator-coupled enhanced transmission through a single subwavelength aperture," *Phys. Rev. Lett.* **102**, 013904 (2009).
11. A. O. Cakmak, K. Aydin, E. Colak, Z. Li, F. Bilotti, L. Vegni and E. Ozbay, "Enhanced transmission through a subwavelength aperture using metamaterials," *App. Phys. Lett.* **95**, 052103 (2009).
12. F. Bilotti, L. Scorrano, E. Ozbay and L. Vegni, "Enhanced transmission through a sub-wavelength aperture: resonant approaches employing metamaterials," *J. Opt. A: Pure Appl. Opt.* **11**, 114029 (2009).
13. F. J. Valdivia-Valero and M. Nieto-Vesperinas, "Resonance excitation and light concentration in sets of dielectric nanocylinders in front of a subwavelength aperture. Effects on extraordinary transmission," *Opt. Express* **18** (7), 6740–6754 (2010).

14. J. B. Pendry, D. Schurig and D. R. Smith, "Controlling electromagnetic fields," *Science* **312**, 1780–1782 (2006).
 15. U. Leonhardt, "Optical conformal mapping," *Science* **312**, 1777–1780 (2006).
 16. D. Schurig, J. B. Pendry and D. R. Smith, "Calculation of material properties and ray tracing in transformation media," *Opt. Express* **14** (21), 9794–9804 (2006).
 17. J. B. Pendry and J. Li, "Hiding under the carpet: A new strategy for cloaking," *Phys. Rev. Lett.* **101** (20), 203901 (2008).
 18. J. B. Pendry, A. J. Holden, W. J. Stewart and I. Youngs, "Extremely low frequency plasmons in metallic mesostructures," *Phys. Rev. Lett.* **76** (25), 4773–4776 (1996).
 19. J. B. Pendry, A. J. Holden, D. J. Robbins and W. J. Stewart, "Magnetism from conductors and enhanced nonlinear phenomena," *IEEE Trans. Microwave Theory Tech.* **47** (11), 2075–2084 (1999).
 20. Y. Zhao, C. Argyropoulos and Y. Hao, "Full-wave finite-difference time-domain simulation of electromagnetic cloaking structures," *Opt. Express* **16** (9), 6717–6730 (2008).
 21. C. Argyropoulos, Y. Zhao and Y. Hao, "A Radially-dependent dispersive finite-difference time-domain method for the evaluation of electromagnetic cloaks," *IEEE Trans. Antennas Propag.* **57** (5), 1432–1441 (2009).
 22. A. Taflov and S. C. Hagness, *Computational electrodynamics: the finite-difference time-domain method (3rd edition)* (Artech House, Boston, 2005).
-

1. Introduction

The extraordinary (optical) transmission (EOT) of electromagnetic waves through periodic arrays of subwavelength holes [1] or slits [2] made in opaque — mostly metallic — screens has been exhaustively studied along the last decade. Comprehensive review papers reporting on the basic physics behind the phenomenon are available nowadays [3–5]. The research of periodic structures has also stimulated the study of the transmission properties through single holes or slits. Sometimes the physics of EOT through periodic structures is closely related with the physics of enhanced transmission through single apertures, as it is the case of slits or holes around which the conducting surface is periodically structured [6–8]. The periodically perforated screen or the periodically structured surface (a metal surface with corrugations, for instance) support surface waves (the so-called *spoof plasmons* [9]) which are strongly excited around certain critical frequencies. However, any other mechanism provoking field enhancement at the aperture level would automatically induce enhanced transmission. Thus, it seems almost obvious that high quality factor resonators placed close to or inside the holes will produce resonant enhancement of the fields and, consequently, enhanced transmission [10, 11]. Other methods have been proposed to enhance transmission of electromagnetic waves through electrically small slits or holes [12, 13].

A common feature to all the methods mentioned in the previous paragraph is their intrinsic narrow band behavior. Narrow bandwidth is associated with the resonant nature of the underlying cause of the phenomenon. A completely different approach is proposed in this contribution. The new approach to obtain extraordinary transmission is based on light squeezing controlled by non-uniform and non-resonant dielectric permittivity distributions around the aperture. Coordinate transformation is applied to design the permittivity distributions and appropriate approximations are introduced to realize a practical all-dielectric device. This design is tested by in-house FDTD based simulations and a great enhancement is verified when the novel devices are applied to the sub-wavelength aperture. Although some frequency dependence of transmissivity is observed, the bandwidth of the relevant enhanced transmission frequency region is much larger than any previously reported.

2. The scheme to enhance the transmission

The method of coordinate transformation offers us an easy way to control the travelling route of the electromagnetic waves [14, 15]. In a Cartesian coordinates, an incident electromagnetic wave travels straightly, while in a distorted coordinates it turns according to the mesh. On the other hand, Maxwell's equations are form-invariant under coordinate transformations [14], and,

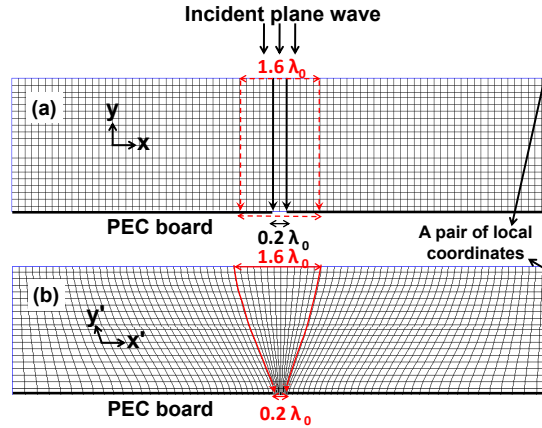


Fig. 1. (a) The space in the Cartesian coordinates. (b) The space in the distorted coordinates.

therefore, one can manipulate the electromagnetic wave in a distorted space by engineering the background with the necessary material parameters.

The main scheme to enhance the transmission through a sub-wavelength aperture is to build a distorted space which can smoothly induce much more energy from a larger aperture into a smaller one. Figure 1(a) shows a space in the Cartesian coordinates. When a plane wave travels into the space from the top, the wave vector k is in the direction towards the bottom along the edge of a grid, as illustrated with black arrows, and so is the Poynting vector S , which represents the flowing of energy. For a perfect electric conductor (PEC) with a $0.2\lambda_0$ (λ_0 the wavelength of free space) wide slit, most incident energy is reflected and little energy could pass through the slit. When the aperture of the slit is enlarged to, for instance, $1.6\lambda_0$, the transmitted energy increases significantly. A distorted space is designed in Fig. 1(b), where the wave vector k is bending towards the slit along the curvature of the grids and the energy is guided from a virtual electrically-large aperture to an electrically-small slit. In this way, the transmission through a sub-wavelength slit could be enhanced dramatically in the distorted space.

A discrete coordinate transformation is used to design the background material for the distorted space. Instead of using the general coordinate transformation in the whole space, the transformation is operated between every pair of local coordinates [17] (a pair of local coordinates is defined as the example in Fig. 1). To simplify the problem, here we only discuss the two dimensional (2D) case with H_x , H_y and E_z components. The Jacobian transformation matrix J is used to map one space to the other. The relative permittivity and permeability values of each block in the distorted space are calculated as [16]

$$\bar{\epsilon}' = \frac{J\bar{\epsilon}J^T}{\det(J)}, \bar{\mu}' = \frac{J\bar{\mu}J^T}{\det(J)} \quad (1)$$

Notice that J is defined for every pair of local coordinates and it has a simpler form in this 2-D case as

$$J = \begin{pmatrix} \frac{\partial x'}{\partial x} & \frac{\partial x'}{\partial y} & 0 \\ \frac{\partial y'}{\partial x} & \frac{\partial y'}{\partial y} & 0 \\ 0 & 0 & 1 \end{pmatrix} \quad (2)$$

A practical way to realize the distorted space is to use an all-dielectric background material. It has been proved that if all the local coordinates in the distorted space are quasi-conformal, the

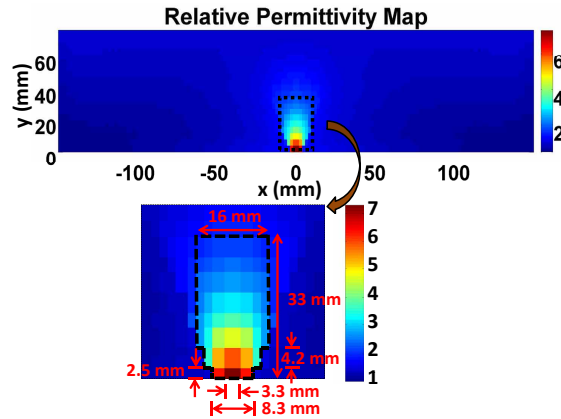


Fig. 2. The relative permittivity map of the distorted space. The dashed black line outlines the profile of the enhancement device.

background permeability could be considered as unity and quasi-isotropic for the E-polarization [17], then, only the permittivity map is required in the z direction. In this scenario, it is difficult to generate a strictly-orthogonal grid to map the distorted space linking the sub-wavelength slit with an electrically large aperture. Instead, very fine meshes are carefully generated in the distorted space to ensure most cells nearly orthogonal, especially in the central region above the slit. Although such an engineering approximation may not represent a mathematically strict transformation, and, hence, is sensitive to wave incident angles for the proposed device, the performance enhancement in terms of extraordinary wave transmission is still evident over a broadband of frequencies, as demonstrated in the following sections.

The relative permittivity (ϵ_r) map is given in Fig. 2. Relative permittivity is very close to unity in most parts of the distorted space, which means most of the background material could be considered as air and dielectrics with varying ϵ_r are mainly required in the central area surrounding the slit. The dashed black line in Fig. 2 outlines the profile of such an enhancement device and the detailed permittivity map. The device has a size of $0.43\lambda_0 \times 0.88\lambda_0$ at 8 GHz.

3. Enhancement performance at a single frequency

FDTD simulations [20, 21] are used to test the performance of the designed device without loss of generality. The operating frequency is set to 8 GHz, the wavelength in free space (λ_0) being 37.5 mm accordingly. The sub-wavelength slit on the PEC plate is $0.2\lambda_0$ (7.5 mm) wide and $0.067\lambda_0$ (2.5 mm) thick. The simulation domain is shown in Fig. 3(a). Periodic boundary conditions (PBC) are applied to realize an incident plane wave with E-polarization impinging from the top. Perfectly matched layers (PML) are added at the left and right sides to eliminate the interference from the neighbours [22]. The amplitude of the electric field is plotted to quantify the distribution of energy. In Fig. 3(a), the incident plane wave irradiates on the PEC plate with the sub-wavelength slit. Extremely low field intensity is observed on the other side of the plate. Figure 3(b) shows the field distribution when the slit is enlarged to be $1.6\lambda_0$ (60 mm) wide. Much energy passes through the slit and propagates further, as expected. When the proposed enhancement device, designed in Fig. 2, is located over the $0.2\lambda_0$ wide slit (inside the region defined by the black lines in Fig. 3(c)), a significant enhancement of the field is observed on the other side of the PEC plate. Ideally, from the point of view of coordinate transformation, the transmitted energy should be the same in (b) and (c). However, the device includes only the central part of the distorted space and the orthogonality in the distorted space is not

guaranteed everywhere. The anisotropic property needs to be included for even enhancing the transmission. Nevertheless, the proposed device still produces strong field enhancement, when comparing Figs. 3(a) and 3(c). A conventional focusing lens is also applied in Fig. 3(d) to compare the performances. The lens has an aperture of $1.6\lambda_0$ and its focal point is set to be at the $0.2\lambda_0$ wide slit to focus more energy directly inside the slit. The transmission through the $0.2\lambda_0$ wide slit increases only slightly. Thus the proposed device outperforms the conventional dielectric lens for field enhancement. Furthermore, the device can be mirrored to the other side of the PEC plate as shown in Fig. 3(f), and the transmitted electromagnetic wave will travel through a second distorted space and leads to much more enhanced field distribution. Fig. 3(e) shows that behind the PEC plate the transmitted wave is constrained in a bundle and high directivity is achieved.

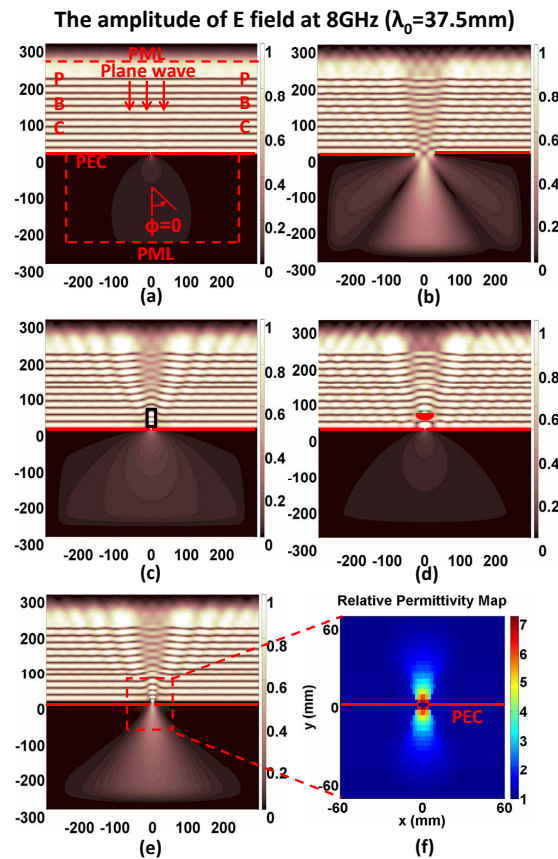


Fig. 3. The amplitudes of the electric field in different cases. (a) The incident plane wave illuminates a PEC plate with a $0.2\lambda_0$ wide slit. (b) The incident plane wave illuminates a PEC plate with a $1.6\lambda_0$ wide slit. (c) The incident plane wave illuminates the above mentioned sub-wavelength slit when the proposed enhancement device is applied in the black lines. (d) The incident plane wave illuminates the sub-wavelength slit after crossing a focusing lens with its focal point located on the slit. (e) The incident plane wave illuminates a PEC plate with a pair of enhancement devices at both sides of the sub-wavelength slit. (f) The permittivity map around the slit in case (e). The map is symmetric.

Radiation patterns are depicted to further compare the field enhancement performances. In Fig. 4(a), the amplitude of E_z is recorded along the semicircle of radius $3\lambda_0$ centered in the slit.

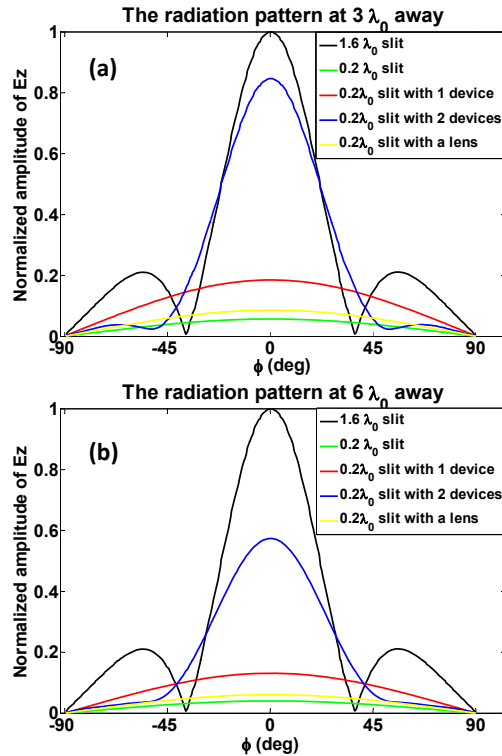


Fig. 4. (a) The radiation pattern recorded at the semicircle $3\lambda_0$ away from the center of the slit. (b) The radiation pattern recorded at the semicircle $6\lambda_0$ away from the center of the slit.

The x axis is the value of ϕ defined in Fig. 3(a). The amplitude of the transmitted E_z field is low when there is only a $0.2\lambda_0$ wide slit on the PEC plate. Once the lens is added, the field increases slightly. However, a significant field enhancement is observed when the proposed device is put above the slit. The amplification at $\phi = 0$ is about 3.25 for amplitude and 10.56 for power. When the mirrored device is added on the other side, the amplification increases remarkably. Around the angle of $\phi = 0$, the E field is not much weaker than that one gets when there is a $1.6\lambda_0$ wide slit on the PEC plate. Note that when the slit is $1.6\lambda_0$ wide, the two side lobes come from the refraction of the PEC plate, which is already observed in Fig. 3(b). Figure 4(b) shows the radiation pattern at the semicircle $6\lambda_0$ away from the center of the slit (far field). The patterns in (b) are similar to the patterns in (a). The amplifications are observed as before while the amplitudes decrease uniformly when the waves travel further.

Figure 5 also shows the energy distribution along the propagation path. The energy is recorded at the direction of $\phi = 0$, from the center of the slit towards the bottom. When the transmitted waves travel to the far field, the enhancement of energy is preserved once the designed device is applied. A pair of devices produce much more transmitted energy than a single one all along the propagation path. Note that the blue curve, which represents the energy when a pair of devices are used, is not smooth from $0.25\lambda_0$ to $0.8\lambda_0$. This area is inside the mirrored device and the reflections between different dielectric blocks are considerable.

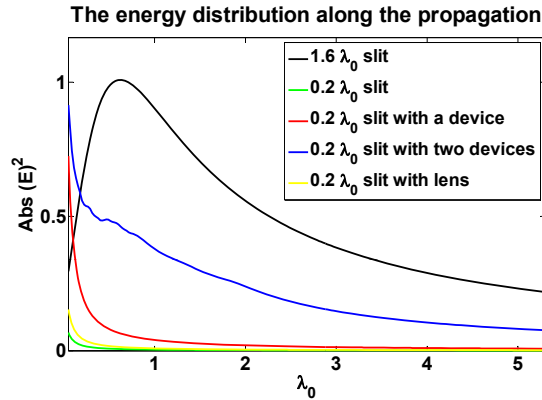


Fig. 5. The energy distribution along the propagation direction. The propagating distance is recorded in terms of the wavelength.

$$\text{Transmitted energy} = \sum \sum S_{\text{through}}$$

$$S_{\text{through}} = E_z \times H_x$$

Fig. 6. Integrate the Poynting vector at the lower surface of the PEC plate over time to get the transmitted energy.

4. The transmitted energy

To quantify the transmitted energy, a broadband Gaussian pulse is applied to excite the slit. Its behaviour in the frequency domain is depicted as the sub-figure in Fig. 7(a) by using Fourier transformation. The Poynting vector over the slit represents the energy passing through. By integrating the Poynting vector at the lower surface of the PEC plate, the total energy transmitted over time is available. Notice that at the lower surface of the PEC plate, only perpendicular electric field and parallel magnetic field exist. So, the transmitted energy could be calculated as shown in Fig. 6. Table 1 gives the values of the transmitted energy in different cases. It is obvious that extremely poor transmission is obtained for the 7.5 mm slit if compared with the energy crossing the 60 mm slit. When a focusing lens is applied, the enhancement is very limited. But once the enhancement device studied in this paper is located above the 7.5 mm wide slit, the transmission increases dramatically (it is about 13 times the energy transmitted without the device). When applying the second device the transmission is further increased (the enhancement factor is about 16). With the implementation of the devices, the transmitted energy increases to about $1/4 \sim 1/3$ of the value when the slit has an aperture of 60 mm. The discrepancy between case 1 and case 4 is due to the fact that the device is mismatched to the free space and the anisotropic material properties is ignored in the design.

5. The broadband performance

To investigate the broadband performance of the devices, an incident pulse spanning from 4 GHz to 8 GHz is applied and the average amplitude of transmitted E_z field at the lines $0.1\lambda_0$ and $3\lambda_0$ (at 6 GHz) away behind the PEC plate is recorded during every time step. The frequency

Table 1. Values of the transmitted energy in different cases

Case No.	The PEC plate with:	Transmitted energy (arb. units)
1	a 60 mm wide slit	965
2	a 7.5 mm wide slit	19
3	a 7.5 mm wide slit and a lens	28
4	a 7.5 mm wide slit and a device	248
5	a 7.5 mm wide slit and a pair of devices	300

domain responses are calculated and plotted in Fig. 7. Slight enhancement is observed at some frequencies, when the conventional lens is used. Once the proposed devices are applied, the transmitted electric field is considerably higher than the values without any devices over the whole frequency domain. When the transmitted waves travel from the very near field of $0.1\lambda_0$ [Fig. 7(a)] to the far field of $3\lambda_0$ [Fig. 7(b)], the significant enhancement is still held. Note that in Fig. 7(a), since the observation line is inside the mirrored device, the case with a couple of devices is not plotted.

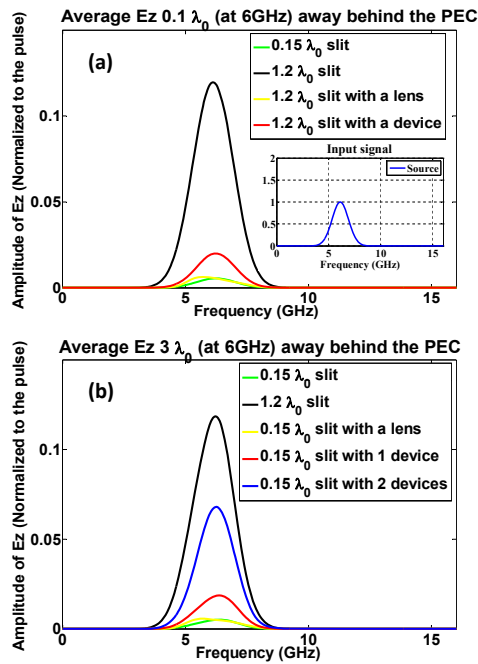


Fig. 7. (a) The average amplitude of E_z field recorded at the line $0.1\lambda_0$ (at 6 GHz) away behind the PEC plate. (b) The average amplitude of E_z field recorded at the line $3\lambda_0$ (at 6 GHz) away behind the PEC plate.

The transmission enhancements produced by the devices and the lens are also calculated and plotted in Fig. 8. The amplitude of electric field is normalized at each frequency point by the value of the green curve, which represents the transmitted field through the sub-wavelength slit without any devices. The results give the detailed information of the amplification and prove that the designed device has significant enhancement performance over a wide frequency range.

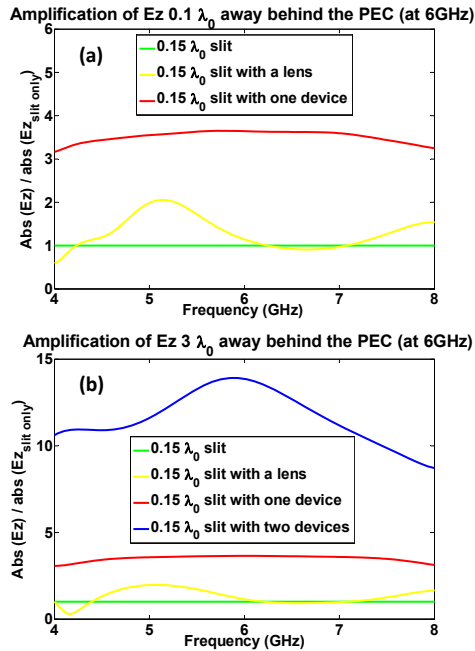


Fig. 8. (a) Amplifications at the line $0.1\lambda_0$ (at 6 GHz) away behind the PEC plate over the frequency spectrum. (b) Amplifications at the line $3\lambda_0$ (at 6 GHz) away behind the PEC plate over the frequency spectrum. The amplitude of electric field is normalized at each frequency point by the value of the green curve (which represents the transmitted field through the sub-wavelength slit) to represent the amplification factor.

6. Conclusion

A device made by dielectric blocks is proposed using the concept of discrete coordinate transformation. Extraordinary transmission in a sub-wavelength aperture is achieved over a broad band from 4 GHz to 8 GHz when the device is applied, thanks to the nonresonant nature of the device. The implementation of a pair of mirrored devices results in even more transmission and higher directivity behind the aperture. FDTD based simulation results have verified the expected performances. The device can be modified to operate for all angles of incidence by rotating the proposed structures. Overall, the device demonstrates superior performance over other existing approaches for broadband extraordinary transmission in a single slit. More importantly, the design based on transformation electromagnetics can be applied to optical frequencies as the required material properties can be easily found from the nature.

Acknowledgments

The authors would like to thank the support of the "Spanish Ministry of Science and Innovation" (Mobility Program, grant number P2009-0405, and Consolider project CSD2008-00066). They'd also thank Mr. C. Argyropoulos for his help during the preparation of the manuscript.